Air-Stable Hexagonal Bipyramidal Dysprosium(III) Single-Ion Magnets with Nearly Perfect D_{6h} Local Symmetry

Zi-Han Li,[a] Yuan-Qi Zhai,[a] Wei-Peng Chen,[a] You-Song Ding,[a] and Yan-Zhen Zheng*[a]

Abstract: *Local eight-coordination of the Dy(III) with D_{6h} symmetry receives much expectation for high-performance single-molecule magnets (SMMs) due to the simultaneous fulfillment of the magnetic axiality and high coordination number (a requisite for the air stability). But the experimental realization is challenging due to the required restriction of six coordination atoms in the equatorial plane of the hexagonal-bipyramid, which is usually too crowded for the central Dy(III) ion. Here we show by using the hexaaza macrocyclic Schiff base ligand and fine-tuning the axial alkoxide/phenol type ligands, a family of hexagonal-bipyramidal Dy(III) complexes, namely [Dy^{III}(L)(Cl)$_2$(H$_2$O/CH$_3$OH)]Cl **1**, [Dy^{III}(L)(C$_6$F$_5$O)$_2$(H$_2$O)](BPh$_4$)·**2**, [Dy^{III}(L)(PhO)$_2$](BPh$_4$) **3**, [Dy^{III}(L)(4-MeO-PhO)$_2$](BPh$_4$) **4**, [Dy^{III}(L)(naPhO)$_2$](BPh$_4$) **5** and [Dy^{III}(L)(Ph$_3$SiO)$_2$](BPh$_4$) **6** (L = (2E,4R,5R,6E,9E,11R,12R,13E)-4,5,11,12-tetraphenyl-3,6,10,13-tetraaza-1,8(2,6)-dipyridina-cyclotetradecaphane-2,6,9,13-tetraene), can be isolated. Among them, complexes **3**, **4** and **5** possess nearly perfect D_{6h} local symmetry. Complex **4** shows the highest effective magnetic reversal barrier 1338 K and an open hysteresis temperature 6 K at the field sweeping rate of 1.2 mT/s, which represents a new record for D_{6h} SMMs.*

Since the mononuclear lanthanide complex (Bu$_4$N)[Tb(Pc)$_2$] reported in 2003, lanthanide-based mononuclear single-molecule magnets (SMMs) have triggered tremendous research interest due to the potential high blocking temperature (T_B), which may bring promising application for high density information storage and miniaturized spintronics.[1,2] In appropriate crystal-field (CF) environment, lanthanide based SMMs have an effective energy barrier for magnetization reversal (U_{eff}) owing to the large angular momentum and strong spin-orbit coupling effect.[3] Recent advances reveal that the control of the coordination environment of the lanthanide is the key for manipulating the CF parameters.[4] It is much governed by the axiality of the crystal field, especially for the dysprosium(III) ion, which has $^6H_{15/2}$ ground term and the energy splitting of eight degenerate Kramers doublets in this ground term. This is well presented in two families of high-performance Dy-based SMMs. One is based on the D_{5h} symmetry,[5] the other is based on cyclopentadienyls ligands.[6] Because Dy(III) has large ionic size,[7] stable Dy(III) complexes have usual 8-9 coordination number. So far, there are only a few air-stable complexes reported in the former family, including the [Dy(bbpen)Br] with U_{eff} larger than 1000 K[8] and [Dy(OPCy$_3$)$_2$(H$_2$O)$_5$]Br$_3$ with an open hysteresis temperature (T_H) higher than 20 K (here T_H is one of the definitions of T_B; the other two popular definitions for T_B are the temperature when the relaxation time reaches 100 second and the peak temperature of the zero-field-cooled (ZFC) magnetization plot).[5c] The latter family is obviously more air sensitive, but performs better in T_B. Thus, ongoing challenge for the latter is rather to improve the stability.

Indeed, dysprosium(III) complexes with D_{6h} symmetry which can simultaneously fulfill the large coordinating number and axial symmetry[9] but it is synthetically challenging to restrict six coordinating atoms in the equatorial plane of the hexagonal-bipyramid.[10] Recently, Murrie *et al* reported the complex [Dy^{III}(L^{N6})(Ph$_3$SiO)$_2$](BPh$_4$) which is close to such a goal,[11] but the Schiff base ligand is not rigid enough and results in a wavy plane.[12] To improve this, we herein use π-conjugated moieties in both axial and equatorial positions, which lead to six air-stable hexaaza macrocyclic complexes, namely [Dy^{III}(L)(Cl)$_2$(H$_2$O/CH$_3$OH)]Cl **1**, [Dy^{III}(L)(C$_6$F$_5$O)$_2$(H$_2$O)](BPh$_4$)·**2**, [Dy^{III}(L)(PhO)$_2$](BPh$_4$) **3**, [Dy^{III}(L)(4-MeO-PhO)$_2$](BPh$_4$) **4**, [Dy^{III}(L)(naPhO)$_2$](BPh$_4$) **5** and [Dy^{III}(L)(Ph$_3$SiO)$_2$](BPh$_4$) **6** (L = (2E,4R,5R,6E,9E,11R,12R,13E)-4,5,11,12-tetraphenyl-3,6,10,13-tetraaza-1,8(2,6)-dipyridinacyclotetradecaphane-2,6,9,13-tetraene). Among them, complexes **3**, **4** and **5** possess nearly perfect hexagonal plane. Magnetic studies reveal that complex **4** shows the highest U_{eff} of 1338 K and T_H of 6 K at the field sweeping rate of 1.2 mT/s, which represents a new record for D_{6h} SMMs.

Our strategy for targeting a hexagonal-bipyramidal dysprosium cation first sought to synthesize a compound of [Dy^{III}(L)Cl$_3$] **1** as a precursor which provides necessary six coordination number on the plane. Then using phenolic or alcoholic ligands can replace chlorides in the precursor; while the large uncoordinated anion BPh$_4^-$ remains in the lattice of **2**-**6** (Scheme 1).

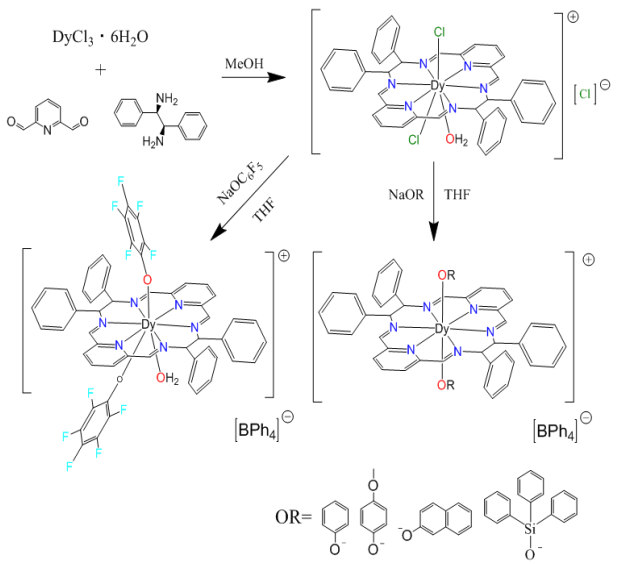

Scheme 1. The preparation route for complexes **1**-**6**. For detailed synthetic procedure, see the Supporting Information.

[a] Frontier Institute of Science and Technology (FIST), Shenzhen Research School, State Key Laboratory for Mechanical Behaviour of Materials, MOE Key Laboratory for Nonequilibrium Synthesis of Condensed Matter, Xi'an Key Laboratory of Sustainable Energy and Materials Chemistry and School of Science Xi'an Jiaotong University, 99 Yanxiang Road, Xi'an, Shaanxi 710054, P. R. China.
Email: zheng.yanzhen@xjtu.edu.cn

Supporting information including experimental details, crystal data and more magnetic studies for this article is available on the WWW under http://www.angewandte.org or from the author.

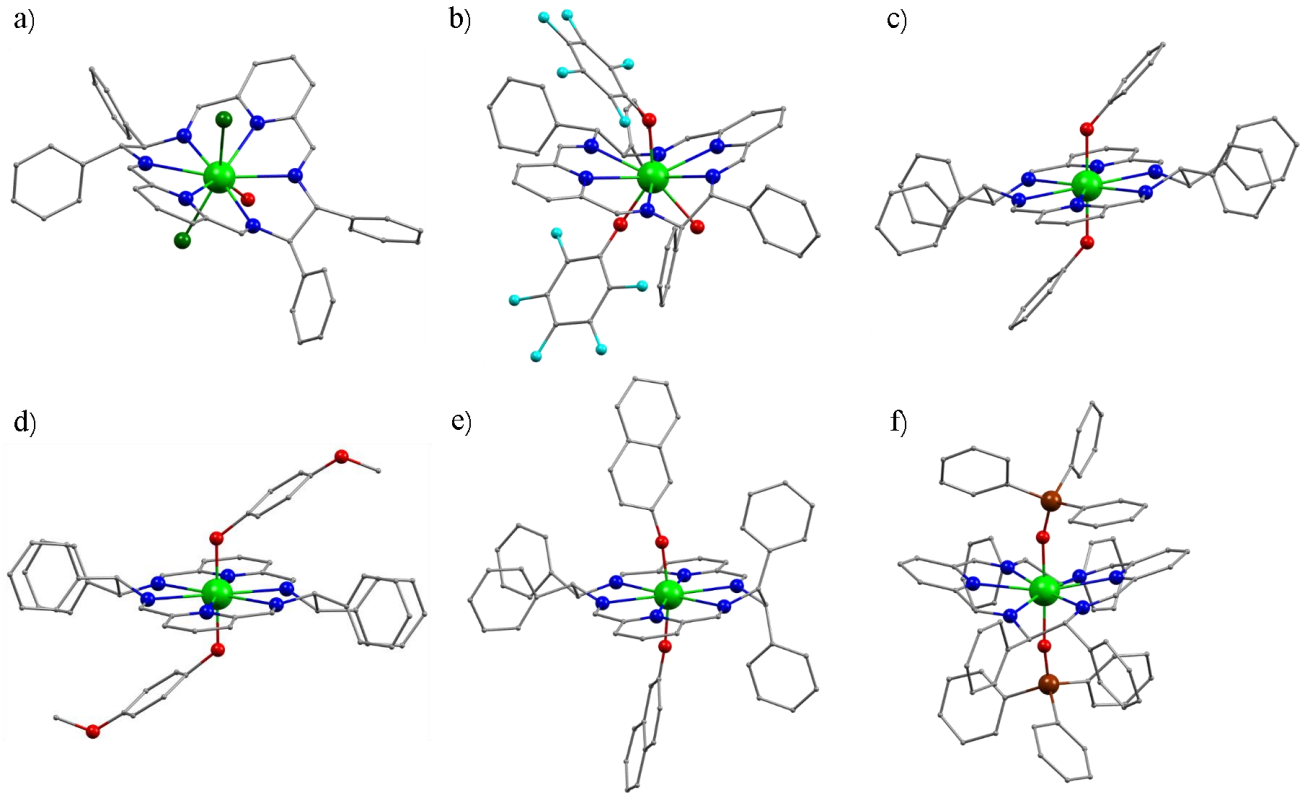

Figure 1. Crystal structure of the $[DyL^{E}L^{A}_{2}(H_2O)_n]^+$ cation in for **1** (a), **2** (b), **3** (c), **4** (d), **5** (e) and **6** (f). Solvent molecules and hydrogen atoms were omitted for clarity. Color codes: Dy, bright green; N, blue; O, red; F, turquoise; Cl, green; C, grey, Si, brown.

Single crystal X-ray diffraction reveals that all six compounds share the formula of $[DyL^{E}L^{A}_{2}(H_2O)_n]^+$ (L^{E} = equatorial Schiff base ligand derived from 2,6-pyridinedicarboxaldehyde and (1R,2R)-(+)-1,2-diphenylethylenediamine; L^{A} = Cl^-, phenolic and alcoholic ligands, n = 1 for **1** and **2**, n = 0 for **3**-**6**) with a charge-balancing anion Cl^- for **1** and BPh_4^- for **2**-**6**.

Complex **1** crystallizes in the monoclinic $P2_1$ space group. There exists two kinds of dysprosium(III) ion in the unit cell. The organic macrocycle surrounds the dysprosium(III) ion with all nitrogen atoms bound to it, while two chloride anions and one water or methanol molecule are connected to the metal center, completing the nine-coordinate sphere (Figure 1a). One free lattice chloride balances the one positive charge of the complex cation, with eight methanol molecules clathrated in the structure.

Complex **2** crystallizes in the orthogonal $P2_12_12_1$ space group. The dysprosium(III) ion is nine-coordinate with two anionic O-donors of pentafluorophenol (Dy-O 2.173(1) Å and 2.191(0) Å), one water molecule (Dy-O 2.435(1) Å), and six N atoms from the macrocycle (Dy-N 2.607(11) Å to 2.745(10) Å, N–Dy–N 59.8(3)° to 61.8(3)°) (Table S4). Note that the N donor atoms of the macrocycle are not coplanar in **2** (Figure 1b).

By replacing pentafluorophenol with phenol and 4-methoxyphenol, the configuration of centural metal ion changed. Complexes **3** and **4** are analogous, both crystallize in the monoclinic *C*2/c space group (Figure 1c and 1d). In these two complexes, the dysprosium(III) ion adopts a near perfect D_{6h} local geometry with six N atoms coordinating in the equatorial plane and two axial O atoms from the phenolic ligands, displaying an essentially linear coordination of the negatively charged donor atoms. The Dy–N distances range from 2.669(5) Å to 2.689(6) Å for **3** and 2.677(6) Å to 2.704(6) Å for **4**. The axial Dy–O distance is 2.108(6) Å for **3** and 2.089(6) Å for **4** with the O–Dy–O angle of perfect 180°. To the best of our knowledge, these Dy-O bonds of complex **4** are the shortest found in high-coordinate (larger than 7) Dy(III) complexes (Table S5). The adjacent N–Dy–N angles are distributed in a very narrow range from 59.62(18)° to 60.46(17)° for **3** and 59.70(17)° to 60.45(17)° for **4** (Table S6-S7), indicating that the six N atoms are arranged in a nearly perfect hexagon. The O-Dy-N angles fall in the range 84.0(2)° to 96.0(2)° for **3** and 87.2(3)° to 93.0(2)° for **4**. Thus, the local coordination symmetry of the Dy(III) ion in **4** is virtually D_{6h}. The configuration is probably as close as ideal hexagonal bipyramid. Continuous shape measure (CShM) analyses using the SHAPE program reveals a slightly compressed hexagonal bipyramidal geometry for **4** (Table S8).[13] In both complexes, the N donor atoms of the macrocycle are coplanar. This could be explained by the steric hindrance of phenolic ligands and intramolecular C-H···π interactions. The short C-H···π interaction of 2.988(5) Å in **3** and 2.948(3) Å in **4** is noteworthy and this interaction is clearly of the H···ring centroid type (θ = 148.3(4)° in **3** and 144.0(1)° in **4**) (Figure S1). When aromatic moieties are introduced, such self-assembly and molecular recognition processes contribute to the coplanarity of six nitrogen atoms.

Complex **5** crystallizes in monoclinic $P2_1/n$ space group with the axial O-Dy-O angle of 168.9°, Dy^{III} site is eight-coordinate with the anionic O-donors of the 2-naphnol having Dy-O bond lengths of 2.100(6) Å and 2.082(6) Å. Whilst the Dy-N bonds fall in the narrow range of 2.654(6) Å - 2.737(7) Å and N–Dy–N angles range from 57.08(19)° to 61.71(19)° (Table S9). The O-Dy-N angles are between 84.9(2)° and 96.0(2)°, stabilizing the compressed hexagonal bipyramidal geometry. There also exists intermolecular and intramolecular C-H···π interactions. The short C-H···π interaction of 2.865(7) Å between THF molecule and naphthol ring (θ = 174.8(7)°), and 2.878(5) Å between two adja-

cent naphthol rings (θ = 130.4(5)°) in packing model is clear (Figure S2).

However, when replacing phenols with alcohols like triphenylsilanol, the configuration of central metal ion changed a little. Complex **6** crystallizes in triclinic *P*1 space group (Figure 1f), and there are four dysprosium(III) ions in the unit cell, albeit their coordination spheres are similar. The dysprosium(III) ion loses the D_{6h} local geometry due to the N_6-donors of the macrocycle. Similar situation can be found in $[Dy^{III}(L^{N6})(Ph_3SiO)_2](BPh_4)$.[11]

Here below we discuss the magnetic properties of complexes **3**, **4** and **5** only, which we found more interesting due to the nearly-perfect D_{6h} local symmetry of the Dy(III) ion. The temperature dependence of magnetic susceptibility under 1000 Oe dc field was measured for the three compounds. The $\chi_M T$ product (in emu K mol^{-1}, and the same below) at room temperature is 13.90, 13.89 and 14.09 for **3**, **4** and **5**, respectively, Those values are slightly lower than the expected value of 14.17 for free Dy(III) ion (S = 5/2, L = 5, g = 4/3). Upon cooling, $\chi_M T$ values are essentially constant, decreasing steadily to 30 K, followed by a sharp decrease at lower temperature and researches 10.46, 9.12 and 8.88 for **3**, **4** and **5**, respectively, at 2 K (Figure S10-S12). The field-dependent magnetization data for these three complexes exhibit continuous increases up to 5.20, 5.46, 5.18 μ_B for **3**, **4** and **5**, respectively (Figure S13-S15). The lack of high-field saturation suggests the presence of significant magnetic anisotropy.

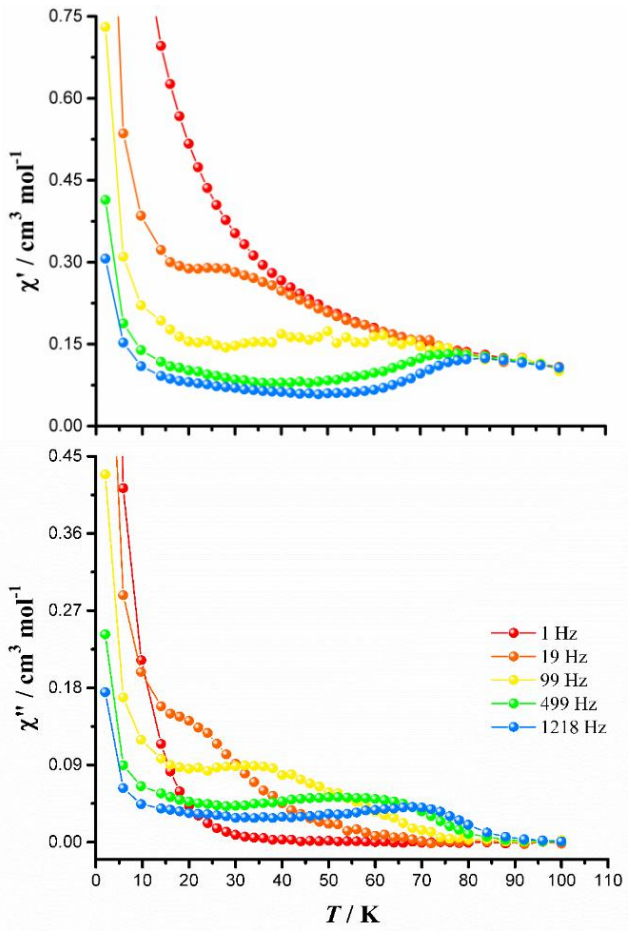

Figure 2. Temperature dependence of the in-phase (upper) and out-of-phase (lower) ac susceptibility in zero dc field, for **4**.

Dynamics magnetic measurements were carried out in zero dc field to probe the slow magnetic relaxation behavior. The temperature and frequency dependences of the in-phase (χ') and out-of-phase (χ'') alternating current (ac) susceptibility components show strong frequency-dependent. The maximum for χ'' (1218 Hz) appears at 60 K for **3**, 70 K for **4** and 62 K for **5**, respectively (Figure 2 and S16-S17). Upon cooling, tails of χ' and χ'' signals are observed, indicating strong tunneling effect. Cole-Cole plots were constructed from these data and fitted to the Debye model to afford the relaxation time (τ) at different temperatures.[14] The equation $\tau^{-1} = \tau_{QTM}^{-1} + CT^n + \tau_0^{-1} \exp(-U_{eff}/T)$ including three possible relaxation processes (QTM, Raman and Orbach mechanisms) was used to analyze the relaxation time.[15] Fitting full temperature range with this equation gives U_{eff} =1100 K for **3** (τ_0 = 9.05(2) × 10^{-12} s, C = 0.090(3) s^{-1} K^{-n}, n = 2.66(4) s, τ_{QTM} = 0.0120(4) s); U_{eff} =1338 K for **4** (τ_0 = 1.85(8) × 10^{-12} s, C = 0.0195(0) s^{-1} K^{-n}, n = 2.82(3) s, τ_{QTM} = 0.131(8) s) and U_{eff} =1226 K for **5** (τ_0 = 1.15(1) × 10^{-12} s, C = 0.0071(5) s^{-1} K^{-n}, n = 3.20(2) s, τ_{QTM} = 0.085(9) s) (Figure 3). Remarkably, the U_{eff} for **4** is the largest known values for all air stable D_{6h} dysprosium SMMs (Table 1).

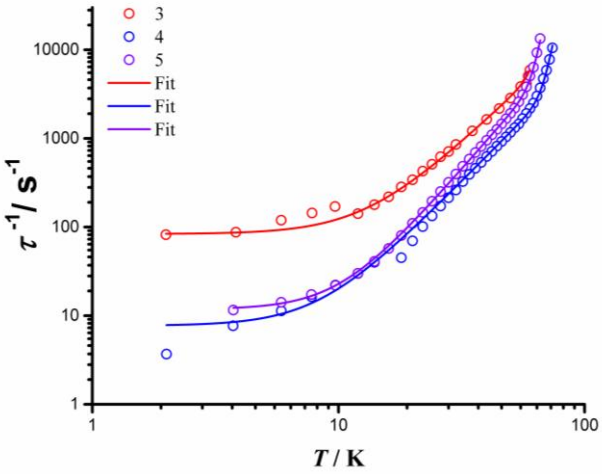

Figure 3. The relaxation time τ^{-1} vs T plot for **3-5** with zero applied field. The solid lines are the best fit of those points, using the equation stated in the text. Color codes: **3**, red; **4**, blue; **5**, violet.

Table 1. The relaxation barriers , CShM value for HBPY-8 and T_H for reported compounds with hexagonal bipyramidal geometry.

Complex	U_{eff} / K	CShM for HBPY-8	T_H (mT s^{-1})	Ref.
$[CeCd_3(Hquinha)_3(n\text{-}Bu_3PO)_2I_3]$	27	0.456	-	10a
$[NdCd_3(Hquinha)_3(n\text{-}Bu_3PO)_2I_3]$	22	0.644	-	10a
$[Yb(NO_3)_3(^tBu_3PO)_2]$	23	0.584	-	10b
$[Dy(^tBu_3PO)_2(NO_3)_3]$	37.1	0.636	-	10c
$[Dy(^tBu_3PO)_2(NO_3)_3]$	46.9	1.108	-	10c
$[Dy(L^{N6})(2,4\text{-di-}^tBu\text{-}PhO)_2](PF_6)$	973	2.472	3(4)	11
$[Dy(L^{N6})(Ph_3SiO)_2](PF_6)$	1080	2.271	3(4)	11
$[Dy(L^{N6})(Ph_3SiO)_2](BPh_4)$	1124	2.163	5(4)	11
3	1100	1.069	2 (1.2)	This work
4	1338	1.028	6 (1.2)	This work
5	1226	1.249	6 (1.2)	This work

To confirm the magnetization blocking, zero-field cooled and field cooled (ZFC-FC) magnetic susceptibility measurements were carried out with 2000 Oe dc field. The ZFC-FC plots show

a divergence at about 6 K and 4 K for **4** and **5**, respectively (Figure S28-S29). The magnetic hysteresis shows butterfly shapes up to 2 K for **3**, 6 K for **4** and **5** with the sweep rate of 12 Oe s^{-1} (Figure 4, S30-S31). As magnetic hysteresis temperature is highly dependent on the field sweep rate and the method of measurement,[16] a further increase in sweep rate to 0.05 T s^{-1} using continuous sweep mode leads to opening of the hysteresis loop of **4** and **5** up to 16 K (Figure S33-S34), which is higher than the T_B of 2.5 K defined by the maximum temperature of the ZFC plot.

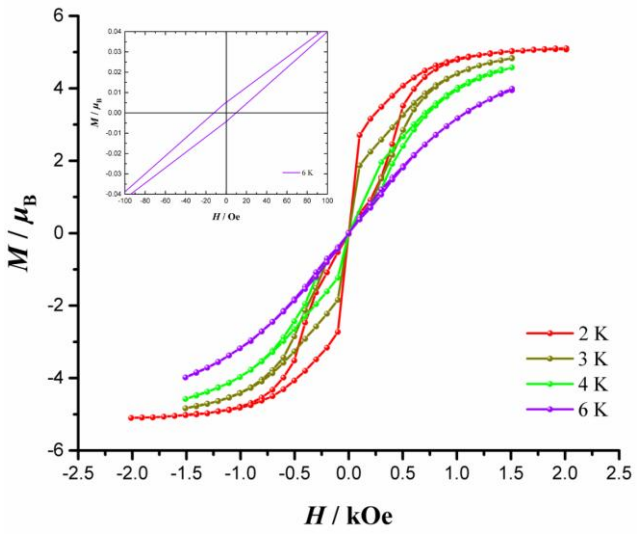

Figure 4. Hysteresis in the *M*(*H*) curve for **4**, collected at temperatures ranging from 2 to 6 K with a 1.2 mTs^{-1} sweep rate. (Inset; expansion of the *M*-*H* curve at 6 K.)

To gain more insight into the magnetic properties of **3-5** on a microscopic scale, we performed ab initio calculations at SA-CASSCF/RASSI level.[17] A highly anisotropic ground Kramer doublet (KD) with $g_z \approx 20$ was obtained for **3-5** and together with second and third KDs were assigned as rather pure m_J = ±15/2, ±13/2 and ±11/2 states respectively, while the other KDs meet with a substantial mixing of magnetic states (Tables S11-S13). Examining the probability of a transition[18] from the first excited m_J = +11/2 state in **3**, we find that quantum tunneling probability to the m_J = -11/2 state is comparable with a phonon-assisted transition to higher KD while it is negligible in **4** and **5**. Other thermal-assisted transitions are detailed in Figure 5a, S35-S36,[19] thus we ascribe the spin dynamic relaxation for **3** happens in-between the third to fifth KDs with the energy 1004 to 1255 K, which is in line with our experimental observed magnetization reversal barrier (1100 K). For **4** and **5**, the predicted barrier is between the fourth and fifth KDs (1511 to 1635 K for **4** and 1426 to 1533 K for **5**), which is a little higher than the U_{eff} (1338 K for **4** and 1226 K for **5**) likely due to presence of anharmonic phonons induced under-barrier spin relaxation that lower U_{eff} in ac susceptibility measurements.[20] The magnetic anisotropy axis for **3-5** is all nearly collinear with the pseudo C_6 axis lying along the axial O-Dy-O bonds (Figure 5b, S37-S38), which indicates a strong crystal field offered by axial ligands and a weak one from the equatorial ligand.[21] Since the nearly perfect hexagonal bipyramidal geometry in **3-5** provide a D_{6h} symmetry we can predict a vanishing QTM effects in the absence of applied field. The crystal field Hamiltonian in D_{6h} symmetry can be simplified by $\hat{H}_{CF} = B_2^0\hat{O}_2^0 + B_4^0\hat{O}_4^0 + B_6^0\hat{O}_6^0 + B_6^6(\hat{O}_6^6 + \hat{O}_6^{-6})$,[22] with removable values of crystal field parameters(CFPs) B_n^q(n = 2, 4 , 6; q ≠ 0) except for B_6^6. Such symmetry efficiently cuts off the majority of unwanted transverse values for crystal field of dysprosium based single ion magnets (SIMs), providing an alternative for QTM mitigating symmetry other than D_{5h} or D_{4d}. As listed in Table 1, complexes **3**-**5** have the most perfect D_{6h} local symmetry among all dysprosium SIMs, which shows us a negligibly QTM transition probability for them (Table S14-S16). By analysing the CFPs, here taking complex **4** as an example, we yield significantly larger axaial CFPs B_n^0(n = 2, 4, 6) than transverse ones, where B_2^0 is six times larger than B_2^2 which suggests a strong uniaxial anisotropy (Table S17). The non-vanishing values for transverse CFPs are coming from slight distortion of the local symmetry and outer uncoordinated atoms, however, relatively small values compared with axial ones are owing to the nearly perfect D_{6h} local symmetry, thus efficiently mitigating QTM and resulting in good SMM behavior in zero field.

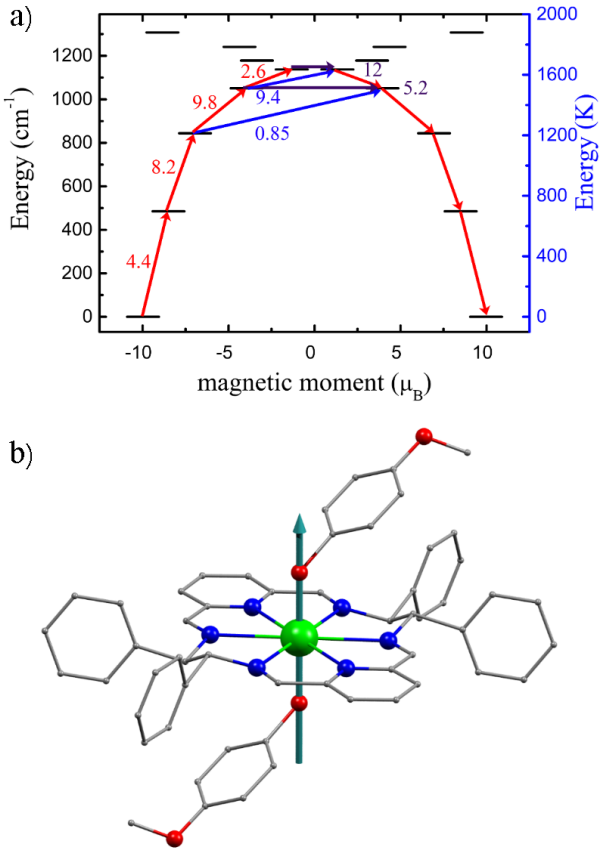

Figure 5. (a) *Ab initio* calculated electronic states of the *J* = 15/2 manifold of the $^6H_{15/2}$ term of Dy^{III} in **4**. Opacity of the arrows give the relative transition propensity. (b) The principal magnetic axis of the ground Kramer's doublet of **4.** Color codes: Dy, bright green; N, blue; O, red; C, grey.

The large difference in the slow magnetization relaxation can be attributed to the change in ligand field around the primary coordination sphere of the Dy(III) ions. By comparing **3** and **4**, the shorter Dy-O bond length of **4** leads to a higher U_{eff} value for **4** than that for **3**. Although the Dy-O bond length for **5** is close to **4**, the O-Dy-O angle is much deviated from 180°. Thus, the U_{eff} for **5** is inferior to **4**. Compared with other compounds with hexagonal bipyramidal geometry, those with six neutral atoms in

the equtorial plane and two negatively charged atoms in the axial direction (see entries 6 to 11 in Table 1), complex **4** is the one has the smallest CShM value, which is probably the reason that **4** has the best performance no matter in U_{eff} or T_H.

In summary, six air-stable macrocyclic Schiff base complexes of dysprosium(III) were obtained. Near perfect D_{6h} local symmetry for the central Dy(III) ion can be generated through intramolecular C-H···π interactions in complexes **3**, **4** and **5**. Complex **4** shows a record smallest CShM value for the ideal D_{6h}-symmetric hexagonal-bipyramidal coordination geometry, which may lead to the largest U_{eff} of 1338 K and a highest open hysteresis temperature of 6 K at the field sweeping rate of 1.2 mT/s for known D_{6h} lanthanide SMMs.

Acknowledgements

This work was supported by NSFC (21871219, 21773130, 21503155 and 21620102002), Key Laboratory Construction Program of Xi'an Municipal Bureau of Science and Technology (201805056ZD7CG40), the China Postdoctoral Science Foundation (2019T120892, 2017M623150 and 2018M631138), the Shaanxi Postdoctoral Science Foundation, Natural Science Basic Research Plan in Shaanxi Province of China (Program No. 2019JQ-292), the Shenzhen Science and Technology Program (JCYJ20180306170859634), China Scholarship Council, Cyrus Chung Ying Tang Foundation and Fundamental Research Funds for Central Universities. We also thank the Instrument Analysis Center of Xi'an Jiaotong University for Dr Huang Chang's assistance with measuring magnetic properties.

Conflict of interest

The authors declare no conflict of interest.

Keywords: dysprosium • hexagonal bipyramidal • single molecule magnets • D_{6h} local symmetry • magnetic properties • ab initio calculations

[1] a) A. Caneschi, D. Gatteschi, R. Sessoli, M. A. Novak, *Nature* **1993**, *365*, 141 - 143; b) F. Troiani, M. Affronte, *Chem. Soc. Rev.* **2011**, *40*, 3119 - 3129; c) L. Bogani, W. Wernsdorfer, *Nat. Mater.* **2008**, *7*, 179 - 186; d) M. Shiddiq, D. Komijani, Y. Duan, A. Gaita-AriÇo, E. Coronado, S. Hill, *Nature* **2016**, *531*, 348 - 351.

[2] N. Ishikawa, M. Sugita, T. Ishikawa, S. Y. Koshihara, Y. Kaizu, *J. Am. Chem. Soc*. **2003**, *125*, 8694 - 8695.

[3] a) J. D. Rinehart, J. R. Long, *Chem. Sci.* **2011**, *2*, 2078 - 2085; b) L. Sorace, C. Benelli, D. Gatteschi, *Chem. Soc. Rev.* **2011**, *40*, 3092 - 3104; c) D. N. Woodruff, R. E. P. Winpenny, R. A. Layfield, *Chem. Rev.* **2013**, *113*, 5110 - 5148; d) P. Zhang, Y.-N. Guo, J. Tang, *Coord. Chem. Rev.* **2013**, *257*, 1728 - 1763; e) S. T. Liddle, J. van Slageren, *Chem. Soc. Rev.* **2015**, *44*, 6655 - 6669.

[4] a) L. Ungur, L. F. Chibotaru, *Inorg. Chem.* **2016**, *55*, 10043 - 10056; b) F. -S. Guo, R. A. Layfield, *Acc. Chem. Res*. **2018**, *51*, 1880 - 1889; c) A. K. Bar, P. Kalita, M. K. Singh, G. Rajaraman, V. Chandrasekhar, *Coord. Chem. Rev*. **2018**, *367*, 163 - 216; d) M. Feng, M. -L. Tong, *Chem. Eur. J.* **2018**, *24*, 7574 - 7594; e) M. Xémard, S. Zimmer, M. Cordier, V. Goudy, L. Ricard, C. Clavaguéra, G. Nocton, *J. Am. Chem. Soc*. **2018**, *140*, 14433 - 14439.

[5] a) Y.-S. Ding, N. F. Chilton, R. E. P. Winpenny, Y.-Z. Zheng, *Angew. Chem. Int. Ed*. **2016**, *55*, 16071 - 16074; b) Y.-C. Chen, J.-L. Liu, Y. Lan, Z.-Q. Zhong, A. Mansikkamaki, L. Ungur, Q.-W. Li, J.-H. Jia, L. F. Chibotaru, J.-B. Han, W. Wernsdorfer, X.-M. Chen, M.-L. Tong, *Chem. - Eur. J.* **2017,** *23*, 5708-5715; c) Y.-C. Chen, J.-L. Liu, L. Ungur, J. Liu, Q.-W. Li, L.-F. Wang, Z.-P. Ni, L. F. Chibotaru, X.-M. Chen, M.-L. Tong, *J. Am. Chem. Soc.* **2016**, *138*, 2829-2837; d) A. B. Canaj, M. K. Singh, C. Wilson, G. Rajaraman, M. Murrie, *Chem Commun*. **2018**, *54*, 8273-8276; e) S. K. Gupta, T. Rajeshkumar, G. Rajaraman, R. Murugavel, *Chem. Sci*. **2016**, *7*, 5181-5191.

[6] a) Y.-S. Meng, Y.-Q. Zhang, Z.-M. Wang, B.-W. Wang, S. Gao, *Chem. - Eur. J.* **2016**, *22*, 12724-12731; b) F.-S. Guo, B. M. Day, Y.-C. Chen, M.-L. Tong, A. Mansikkamäki, R. A. Layfield, *Angew. Chem. Int. Ed*. **2017**, *56*, 11445 - 11449; c) C. A. P. Goodwin, F. Ortu, D. Reta, N. F. Chilton, D. P. Mills, *Nature* **2017**, *548*, 439 - 442; e) F.-S. Guo, B. M. Day, Y.-C. Chen, M.-L. Tong, A. Mansikkamäki, R. A. Layfield, *Science* **2018**, *362*, 1400 - 1403; f) K. R. McClain, C. A. Gould, K. Chakarawet, S. J. Teat, T. J. Groshens, J. R. Long, B. G. Harvey, *Chem. Sci*. **2018**, *9*, 8492 - 8503.

[7] a) J.-C. G. Bünzli, *J. Coord. Chem.* **2014**, *67*, 3706 - 3733; b) J. Zhang, N. Heinz, M. Dolg, *Inorg. Chem.* **2014**, *53*, 7700 - 7708; c) A. B. Canaj, M. K. Singh, E. R. Marti, M. Damjanović, C. Wilson, O. Céspedes, W. Wernsdorfer, G. Rajaraman, M. Murrie, *Chem. Commun*. **2019**, 55, 5950 - 5953.

[8] J. Liu, Y.-C. Chen, J.-L. Liu, V. Vieru, L. Ungur, J.-H. Jia, L. F. Chibotaru, Y. Lan, W. Wernsdorfer, S. Gao, X.-M. Chen, M.-L. Tong, *J. Am. Chem. Soc.* **2016**, *138*, 5441 - 5450.

[9] a) C. Goŕller-Walrand, K. Binnemans, *Handbook on the Physics and Chemistry of Rare Earths* **1996**, *23*, 121; b) B. Bleaney, K. W. H. Stevens, *Rep. Prog. Phys*. **1953**, *16*, 108.

[10] a) Q. -W. Li, R.-C. Wan, Y. -C. Chen, J. -L. Liu, L.-F. Wang, J. -H. Jia, N. F. Chilton, M. -L. Tong, *Chem.Commun*. **2016**, *52*, 13365 - 13368; b) W. Zhao, H. Cui, X.-Y. Chen, G. Yi, L. Chen, A. Yuan, C.-L. Luo, *Dalton Trans*. **2019**, *48*, 5621 – 5626; c) J. Li, S. Gomez-Coca, B. S. Dolinar, L. Yang, F. Yu, M. Kong, Y.-Q. Zhang, Y. Song, K. R. Dunbar, *Inorg. Chem.* **2019**, *58*, 2610 – 2617.

[11] A. B. Canaj, S. Dey, E. R. Marti, C. Wilson, G. Rajaraman, M. Murrie, *Angew. Chem. Int. Ed.* 10.1002/anie.201907686.

[12] a) J. Lisowski, J. Mazurek, *Polyhedron.* **2002**, *21*, 811 - 816; b) J. Gregoliński, A. Kochel, J. Lisowski, *Polyhedron.* **2006**, 25, 2745 – 2754; c) G. Bombieri, F. Benetollo, A. Polo, L. De Cola, D. L. Smailes, L. M. Vallarino, *Inorg. Chem.***1986**, *25*, 81127 - 81132; d) P. H. Smith, J. R. Brainard, D.E. Morris, G. D. Jarvinen, R. R. Ryan, *J. Am. Chem. Soc.***1989**, *111*, 197437-197443.

[13] a) M. Llune, D. Casanova, J. Cirera, J. Bo, P. Alemany, S.Alvarez, SHAPE (Version 2.1), Barcelona, 2013; b) D. Casanova, M. Llunell, P. Alemany, S. Alvarez. *Chem. Eur. J*. **2005**, *11*, 1479 - 1494.

[14] D. Gatteschi, R. Sessoli, J. Villain in *Molecular Nanomagnets*, Oxford Univ. Press, **2006**.

[15] Y.-S. Ding, K.-X. Yu, D. Reta, F. Ortu, R. E. P. Winpenny, Y.-Z. Zheng, N. F. Chilton, *Nat. Commun.* **2018**, *9*, 3134.

[16] J.-L. Liu, Y.-C. Chen, M.-L. Tong, *Chem. Soc. Rev*. **2018**, *47*, 2431 - 2453.

[17] a) F. Aquilante, J. Autschbach, R. K. Carlson, L. F. Chibotaru, M. G. Delcey, L. De Vico, I. Fdez Galvan, N. Ferre, L. M. Frutos, L. Gagliardi, et al., *J. Comput. Chem*. **2016**, *37*, 506; b) L. F. Chibotaru, L. Ungur, *J. Chem. Phys*. **2012**, *137*, 064112; c) A. A. Granovsky, *J. Chem. Phys.* **2011**, *134*, 214113.

[18] a) R. J. Blagg, L. Ungur, F. Tuna, J. Speak, P. Comar, D. Collison, W. Wernsdorfer, E. J. L. McInnes, L. F. Chibotaru, R. E. P. Winpenny, *Nat. Chem*. **2013**, *5*, 673 - 678; b) N. F. Chilton, C. A. P. Goodwin, D. P. Mills, R. E. P. Winpenny, *Chem. Commun*. **2015**, *51*, 101 - 103.

[19] N. F. Chilton, *Inorg. Chem*. **2015**, *54*, 2097 - 2099.

[20] A. Lunghi, F. Totti, R. Sessoli, S. Sanvito, *Nat. Commun*. **2016**, *8*, 14620.

[21] L. Ungur, L. F. Chibotaru, *Phys. Chem. Chem. Phys*. **2011**, *13*, 20086 - 20090.

[22] J. J. Le Roy, L. Ungur, I. Korobkov, L. F. Chibotaru, *J. Am. Chem. Soc.* **2014**, 136, 8003 - 8010.

.